Feasibility Study of Onboard PV for Commercial Vehicle Application: Analysis for the Effects of PV Systems in Different Use Cases Using a PVEV Simulator

Shuai Pei[1], Jingxuan Peng [1], Kimiyoshi Kobayashi[1], Toshio Hirota[1], Yushi Kamiya[1], Hidenori Mizuno[2], Takashi Oozeki[2]

[1] *Waseda University, Tokyo, Japan,*
Shuai Pei (corresponding author), peishuai@fuji.waseda.jp

[2] *National Institute of Advanced Industrial Science and Technology (AIST), Fukushima Prefecture, Japan*

Executive Summary

The performance of photovoltaic electric vehicles (PVEVs) varies significantly depending on use cases, driving conditions, and weather conditions. In this study, we conducted vehicle field tests for various EV use cases, including an urban delivery van, a community bus in hot spring areas and mountainous roads. Based on the test results, we developed a high-precision EV electric consumption (EVEC) model and an energy balance model capable of predicting PV generation, then the accuracy verification for them was conducted. The results suggest that the PV system's effectiveness is particularly high for the urban delivery van with short driving distances and the community bus in hot spring areas. Although performance declined in all use cases during winter, it is possible to significantly improve the performance of PVEVs in winter by using heaters strategically.

Keywords: Electric Vehicles, Modelling & Simulation, Energy Management, Sustainable Energy, Drive & Propulsion Systems

1 Introduction

Photovoltaic electric vehicles (PVEVs) are equipped with solar power systems that enable them to operate on self-generated electricity. In addition to reducing environmental impact, these vehicles offer significant practical advantages by drastically cutting the energy and frequency of grid-based plug-in charging [1][2]. Recent advancements in photovoltaic and battery technologies have rapidly increased the feasibility of PVEV implementation [3]. Consequently, it is essential to analyze how driving conditions and weather variations affect vehicle performance across various use cases, thereby clarifying both the benefits and the challenges of this emerging technology.

In this study, we focus on clarifying the differences in PV integration effects across various applications, vehicle types, and driving conditions, and we aim to propose practical implementation directions for

PVEVs based on these factors. Three use cases in Fukushima Prefecture, Japan, were analyzed: (1) a community bus (CBus) operating in residential and mountainous areas (Tatsugoyama Route, TY. Rt.), (2) a CBus serving a hot spring area (Iizakaonsen Route, IO. Rt.), and (3) a small delivery vehicle (DVan) operating in the urban area of Koriyama City, Fukushima Prefcture (Koriyama Route, KY. Rt.). Real-world vehicle tests and simulation models were employed for analysis. In the vehicle tests, equipment for measuring EV electric consumption (EC) and solar irradiance was installed, enabling the collection and analysis of real-world driving data. Based on the test results, an EV EC model and an energy balance model capable of predicting PV generation were developed and validated. Subsequently, using the developed simulation model, we analyzed the performance of PVEVs in each use case and identified key impacting factors as the general, such as vehicle weight, average speed, road slope, acceleration and deceleration, ambient temperature, auxiliary system (AUX) power consumption, solar altitude, shading, as the general theory. A key indicator, the PV coverage rate, defined as the ratio of PV generation to EV EC, was estimated to represent the effectiveness of PV system installation. Furthermore, the study examined potential improvements in the PV coverage rate through wise use of the air-conditioning system.

2 Vehicle Field Tests and Data Analysis
2.1 Overview of vehicle field tests

The overview of each vehicle for the field tests is shown in Table 1. The CBus is based on the Toyota Hiace Super Long Hi-Roof, with a vehicle mass of 2165 kg. The engine, transmission, and propeller shaft were removed from the front, and a traction motor with a reduction gear was installed on the rear axle. The motor has a maximum output of 140 kW and a rated output of 75 kW. Its vehicle power battery, operating at 350 V with a capacity of 39.4 kWh, was divided into three packages and mounted beneath the floor. In the front engine compartment, auxiliary component including a junction box, a 12 V auxiliary battery, a DC/DC converter, and an air conditioning compressor were installed. The vehicle is equipped with both standard 200 V charging and fast charging ports. It features a reduction ratio of 10.8 and tires sized 195R15. For solar irradiance measurements, a roof carrier was fitted with two small PV module-based irradiance sensors, a PV panel to power the measurement system, a temperature sensor, and a GPS sensor. The DVan is based on the Mitsubishi Minicab MiEV and is equipped with measurement equipment mounted on the roof. It has an empty weight of 1,100 kg, a seating capacity for 2 crew, and a total loaded weight of 1,210 kg. The reduction gear is with a reduction ratio of 7.065 and tires sized

Table 1: Main specs of vehicles tested in various use cases

Class	Items	Unit	Use case 1A / 1B	Use case 2A
	Veh. Name	-	Community bus (CBus)	Delivery van (DVan)
Vehicle	Appearance	-		
	Veh. Mass	kg	2165	1100
	Passenger Capa.	person	10	2
	Max. load Capa.	kg	-	370
	Gross Mass	kg	2715	1210
Mot. & Inv.	Max Torque	Nm	275	196
	Max Power	kW	140	30
	Rated Power	kW	75	25
	Mot. & Inv. Efficiency	%	90 (presumed)	90 (presumed)
Dri	Gear Ratio	-	10.8	7.065
	Tire	-	195R15	145R12
Bat	Capacity	kWh	39.4	16
	OCV	V	350	350

145R12. The motor delivers a maximum output of 30 kW and a rated output of 25 kW, while the battery has a capacity of 16 kWh.

The tests routs and their features of 3 use cases are shown in Table 2 and Figure 1. In the CBus (TY. Rt.) test, the vehicle operated in residential areas, including mountainous roads, on a 24 km round-trip route with 3 trips per day: Trip 1 and Trip 2 from 10:00 to 12:00, and Trip 3 from 13:00 to 14:00, over a 9-month period from June 2022 to February 2023, averaging 15 days per month for a total of 127 days and approximately 9,000 km. In the CBus (IO. Rt.) test, the vehicle operated in a hot spring area on a 6 km round-trip route with 6 trips per day: Trips 1 to 3 from 9:00 to 11:00 in the morning, and Trips 4 to 6 from 13:00 to 15:00 in the afternoon, over a 6-month period from September 2023 to February 2024, totaling 108 days and approximately 3,600 km. The "trip" is defined as the period from the moment the shift lever switches to D immediately before departure until it changes to N immediately before parking

Table 2: Tests and routs features of various use cases

Items	Unit	Use case 1A	Use case 1B	Use case 2A
Vehicle for tests	-	Community bus (CBus)	Community bus (CBus)	Delivery van (DVan)
Route name	-	Tatsugoyama (TY. Rt.)	Iizakaonsen (IO. Rt.)	Koriyama (KY. Rt.)
Use & purpose		Residential commuting	Hot spring area shuttle	Supermarket delivery
Gross test days	day	127	108	695
Gross test distance	km	>9000	>3600	>9300
Trips per day	trip	3	6	11 (annual ave.)
Distance per trip	km	24.5	5.6	1.3
Ave speed	km/h	25.3	14.7	14.9
Trip time	min	58.2	22.5	5.0 (annual ave.)
stop time for delivery	min	-	-	5.2 (annual ave.)
Accum. uphill height	m/km	23.1	10.8	6.0
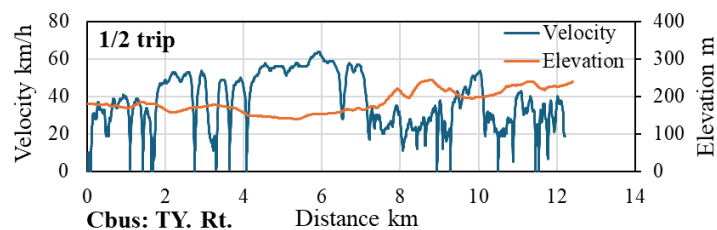
(a) CBus (TY. Rt.)
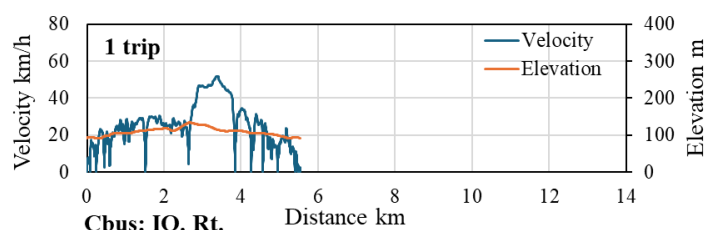
(b) CBus (IO. Rt.)
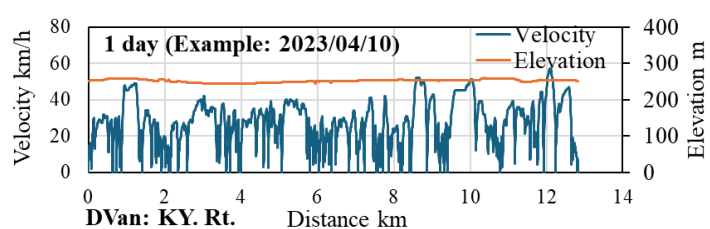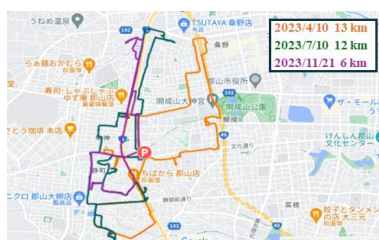
(c) DVan (KY. Rt., represetative)

Figure 1: Routs map, velocity, elevation features in 3 use cases

at the destination. The DVan (KY. Rt.) was utilized for parcel delivery operations from a supermarket with a non-fixed route. After plug-in charging starting at 8:00 in the morning, the vehicle departed from the supermarket at approximately 13:30, operating for around 2 hours with roughly 10 trips and 10 stops for delivery. The average trip duration was 5 mins, and the average delivery stop lasted 5.2 mins. Over a 35-month period from February 2022 to December 2024, tests were conducted in 695 days, with an average daily travel distance of 13.5 km, an average trip distance of 1.3 km. During the 3 vehicle field tests, EV EC data and solar irradiance data were collected. As illustrated in the Figure 1and Table 2, although the same test vehicles (CBus) were used for both TY. Rt. and IO. Rt., TY. Rt. has an average speed of 25.3 km/h, which is considerably faster than the 14.7 km/h observed on the IO. Rt. route. The TY. Rt. route includes mountainous roads with steep slopes, on which there is an accumulated uphill height of 23.1 m/km. The DVan (KY. Rt.) primarily traverses urban areas with some arterial roads, featuring minimal elevation changes and gentle slopes; however, its operation for supermarket parcel delivery is characterized by long stop durations for deliveries.

2.2   Vehicle field test data analysis
2.2.1   EV EC characteristics

Figure 2 shows the EV EC rate per trip for different ambient temperatures across the use cases. Figure 2(a) compares EV EC rate of CBus (TY. Rt.) and CBus (IO. Rt.). Under conditions around 20 degC of ambient temperature, where minimal air conditioning operation is assumed, the EV EC rate on the TY. Rt. (blue plot) is 210 Wh/km, whereas that on the IO. Rt. (orange plot) is 180 Wh/km. In cold conditions (around 0 degC), the EC rate increases to approximately 330 Wh/km for the TY. Rt. and about 380 Wh/km for the IO. Rt. Figure 2(b) compares CBus (IO. Rt.) and DVan (KY. Rt.)'s EV EC rate under different ambient temperatures. The EV EC rate of DVan (KY. Rt.) is lower to around 140 Wh/km when minimal air conditioning operation (around 20 degC) compared to CBus (IO. Rt.)'s 180 Wh/km of EV EC rate. However, the EC rate of DVan (KY. Rt.) sharply increases to approximately 610 Wh/km with around 0 degC, which is 336% higher than the lowest EV EC rate. Figure 3 compares the driving EC rate across the 3 use cases. The average EC rate for CBus (TY. Rt.), CBus (IO. Rt.), and DVan (KY. Rt.) are approximately 200, 150, and 100 Wh/km. In addition, the variation in driving EC rate with ambient temperature changes differs among the use cases, with temperature coefficients of about -1, -1.5, and -0.5 Wh/km/degC, respectively. Figure 4 illustrates the impact of ambient temperature on the AUX power dominated by the air-conditioning system. For CBus (KY. Rt. & IO. Rt.), the PTC heater is activated at around 17°C under cold conditions, with its average output increasing as the temperature decreases, reaching maximum values of approximately 4.4 kW for KY. Rt. and 3 kW for IO. Rt. DVan's PTC heater is activated at around 15°C, with a maximum average output of about 2.9 kW. In all 3 use cases, the cooler starts operating at around 23°C, and its output increases with rising temperatures, reaching a maximum average output of 2 kW.

By comparing the 3 use cases, it can be considered that the lower driving EC rate for DVan (KY. Rt.) is attributable to its gentle road slope and lower average velocity. Ambient temperature affects driving EC rate by influencing rolling and air resistance. The larger absolute temperature coefficient for the driving EC rate of CBus (IO. Rt.) is due to its route having a less steep slope than TY. Rt. and a heavier vehicle weight than DVan, which increases the contribution of rolling resistance. The variation in overall vehicle EC rate, which includes AUX impact due to ambient temperature changes, is greatest for DVan (KY. Rt.) and smallest for CBus (TY. Rt.). The larger change observed in CBus (IO. Rt.) compared to CBus (TY. Rt.) is attributed to the significant impact of the PTC heater during cold conditions. On the IO. Rt., the lower average velocity results in higher PTC heater EC per unit distance. As shown in Figure 5, during delivery stops, significant time is spent unloading cargo or handing it over to customers, during which the vehicle is often left in the Key-on state. In a typical day, delivery stops spend a total of 82 mins compared to 51mins of trips, and heater EC during delivery stops accounts for 54% of the total heater EC. This is considered the primary reason for the greatest variation in vehicle EC for DVan (KY. Rt.). In cold winter conditions, especially at low speeds and during long-time idling, AUX EC further increases the overall vehicle EC.

(a) CBus (TY. Rt.) Vs CBus (IO. Rt.)   (b) CBus (IO. Rt.) Vs DVan (KY. Rt.)

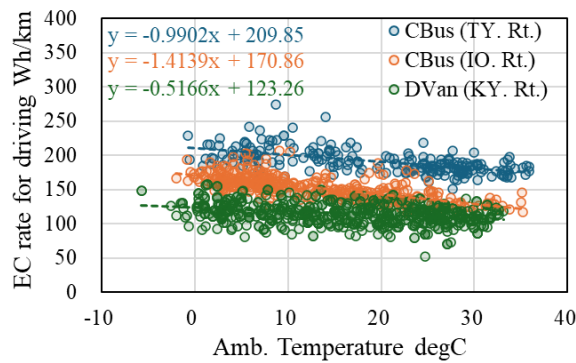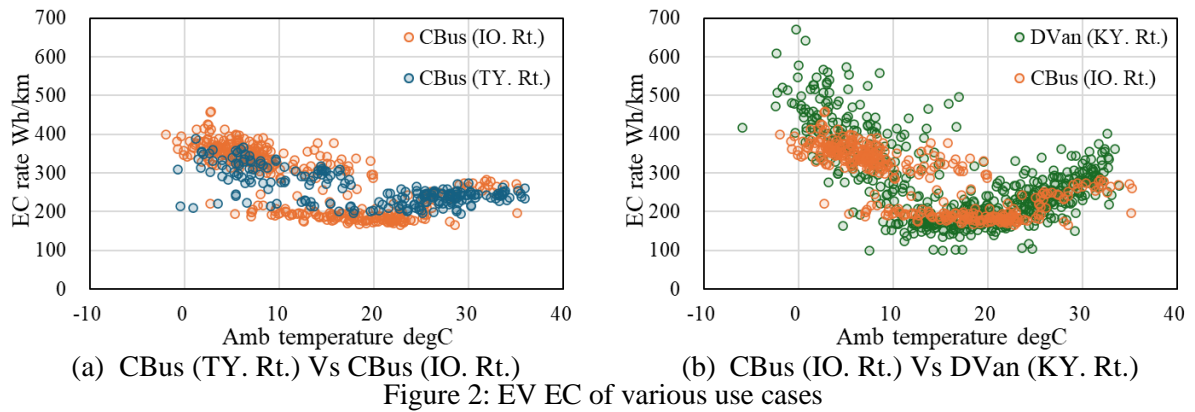Figure 2: EV EC of various use cases

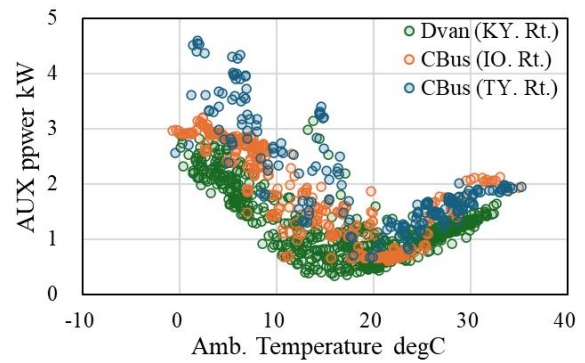Figure 3: EC for driving of various use cases   Figure 4: PV power of various use cases
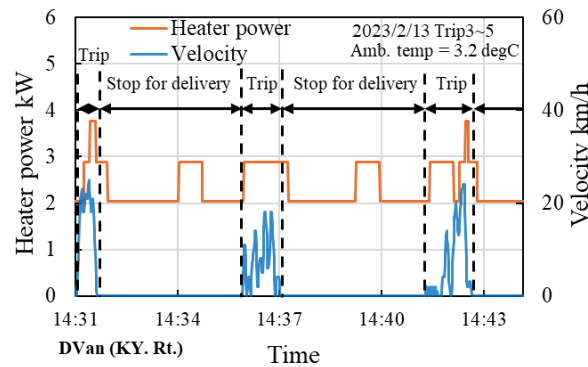

Figure 5: Heater power for DVan when idling (Ex. of Feb. 13, 2023)

2.2.2 Solar irradiance and V/F value

Figure 6 and Figure 7 presents the fixed-point irradiance, the vehicle irradiance and V/F values for DVan (KY. Rt.), which are the daily average values for every month when the DVan (KY. Rt.) tests conducted. In addition, due to DVan (KY. Rt.)'s tests covered a long-term period of 35 months from February 2022 to December 2024, the data in 2023 was summarized as a representative result. The fixed-point irradiance is defined as the solar irradiance reaching the ground and regarded as under no-shade conditions, using the 1-hour global horizontal irradiance (GHI) data for Fukushima City from the Japan Meteorological Agency (JMA) database, due to the irradiance data is not open for Koriyama City in JMA database. There is around 42.5 km from Fukushima station to the starting point for the operation in KY. Rt. The vehicle irradiance is the measured value obtained from the on-board irradiance sensor. The V/F value, defined as the ratio of vehicle irradiance to fixed-point irradiance, quantifies the impact of shade, which is caused by surrounding buildings, trees, pedestrian overpasses, traffic signs, etc. The distance of 42.5 km between Fukushima City and KY. Rt. may lead to slight fluctuation of V/F value because of the different clouds hovering conditions. The Fixed-point irradiance of DVan (KY. Rt.) varies from 2.0 (Jan.) to 5.6 kWh/m2/day (Aug.), and DVan (KY. Rt.) exhibits high V/F values of nearly 80%~90% throughout the year, which means 80%~90% of the fixed-point irradiance can reach the PV panel in every month in 2023,

under the impact of shades surrounding the vehicle.

The photos describing the sky conditions were taken to analyze the effects caused by shades of buildings and trees, etc. surrounding the vehicles. Figure 8 presents hemispherical images taken at the parking lots and along representative driving routes for DVan (KY. Rt.). When the vehicle irradiance reaches the PV panel from the fixed-point irradiance, solar irradiance (GHI) comprises 3 components: direct normal irradiance (DNI), diffuse horizontal irradiance (DHI), and reflected irradiance [4]. If the solar altitude is lower than the elevation angle (shade height) of buildings or other structures, the DNI becomes 0, leaving the DHI as the dominant contributor and causing a significant decrease in the V/F value. The left hemispherical images (Figure 8(a)), captured during parking, display a horizontal axis covering 360° around the vehicle, centered on the south, and a vertical axis ranging from the horizontal plane of the PV panel up to 90° at the zenith and down to -30° below the horizontal. The shade heights on the east side are approximately 15~20°, and on the west side they are around 10~15°. The average shade height over the full 360° surrounding is about 15°. The orange, blue and light blue lines represent the solar trajectory throughout the day for the summer solstice, the spring (fall) equinox, and the winter solstice, respectively. On the summer solstice, from sunrise at 4:25 until about 6:30 (hour angle -80°) and from approximately 18:30 (hour angle 100°) until 19:00 at sunset, the solar altitude remains below the elevation angles of the yellow building on the east side and the distant white building on the west, causing the sun to be obscured by these structures. However, On the winter solstice, the period during which the solar altitude is below
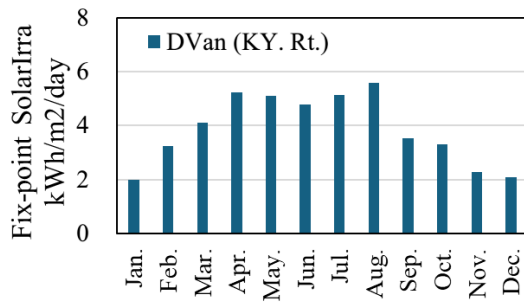

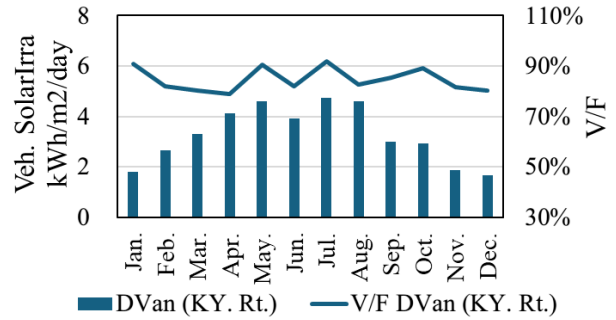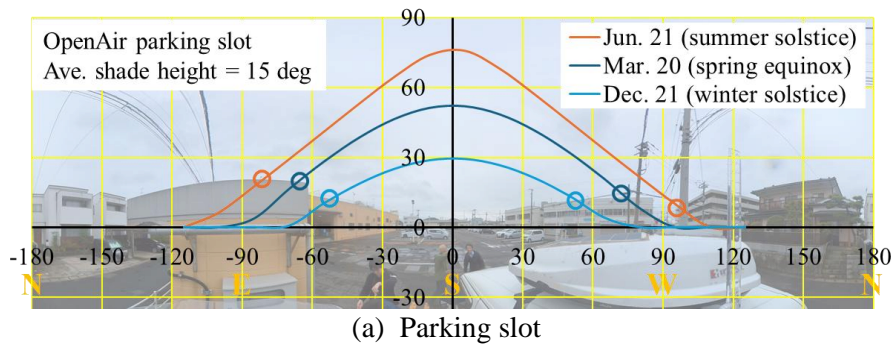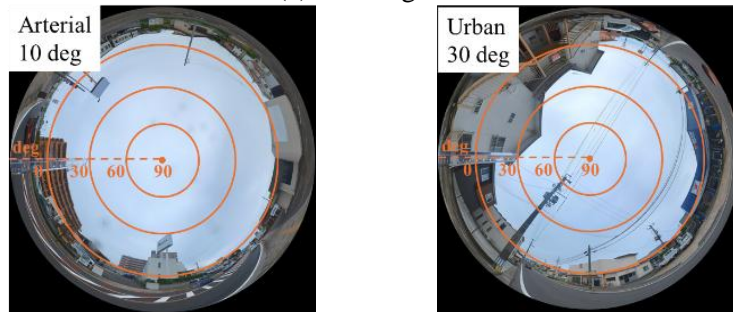Figure 6: Fixed-point irradiance
for DVan (KY.Rt.)

Figure 7: Vehicle irradiance and V/F
for DVan (KY.Rt.)

(a) Parking slot

(b) Route

Figure 8: Shade height in parking slot and route for DVan (KY.Rt.)

the shade height extends from sunrise at 6:47 until about 8:00 in the morning and from around 15:30 until 16:31 at sunset, which means the period of the sun is obscured is longer than it on the summer solstice. Figure 8(b) shows the sky hemispherical images captured when driving on arterial and urban roads. The same as Figure 8(a) taken at the parking slot, in Figure 8(b) the PV panel's horizontal plane is set at 0°, with the zenith at 90° (center of the image) and the lower limit at -30° (edge of the image). The average shade heights for arterial and urban roads are about 10° and 30°. The solar altitude varies intensity throughout different seasons and time of day, as explained above, the V/F value can be significantly impacted by the shade at parking slot and along the road, in the seasons and time of day when the solar altitude is low. The fixed-point irradiance at 10:00~14:00 occupies about half of the total irradiance in a day [4]. As for DVan (KY. Rt.), the operation period is 13:30~15:30, which slips out of the period of peak irradiance, so the average height at parking slot primarily impacts the V/F of DVan (KY. Rt.). Furthermore, according to the results of the hemispherical images analysis above, the period when the sun is obscured by the buildings at east and west side surrounding the vehicle is before 6:30 or after 18:30 for summer, and before 8:00 and after 15:30 for winter. This period is very close to the sunrise and sunset, when the irradiance is not strong, benefited from the relatively low average shade height at parking slot. Thus, it can be considered that the shading effect on DVan (KY. Rt.) is minimal, allowing its V/F value to remain at a high level of 80~90% throughout the year.

3 Simulation Model

To analyze the PV integration effects for each use case and their influencing factors, an EV EC model and an energy balance model, which is capable of predicting PV generation and the ratio of PV generation to EV EC, were developed based on the analysis of vehicle test data.

The flowcharts of the EV EC model and the energy balance model are shown in Figure 9(a) and (b). In the EV EC model, the key vehicle specifications and AUX power settings were established based on the test data for each use case. The road slope calculated from vehicle speed and elevation data (using data from the Geospatial Information Authority of Japan) and the ambient temperature are input into the EV EC model to calculate driving resistances, including rolling resistance, aerodynamic drag, acceleration

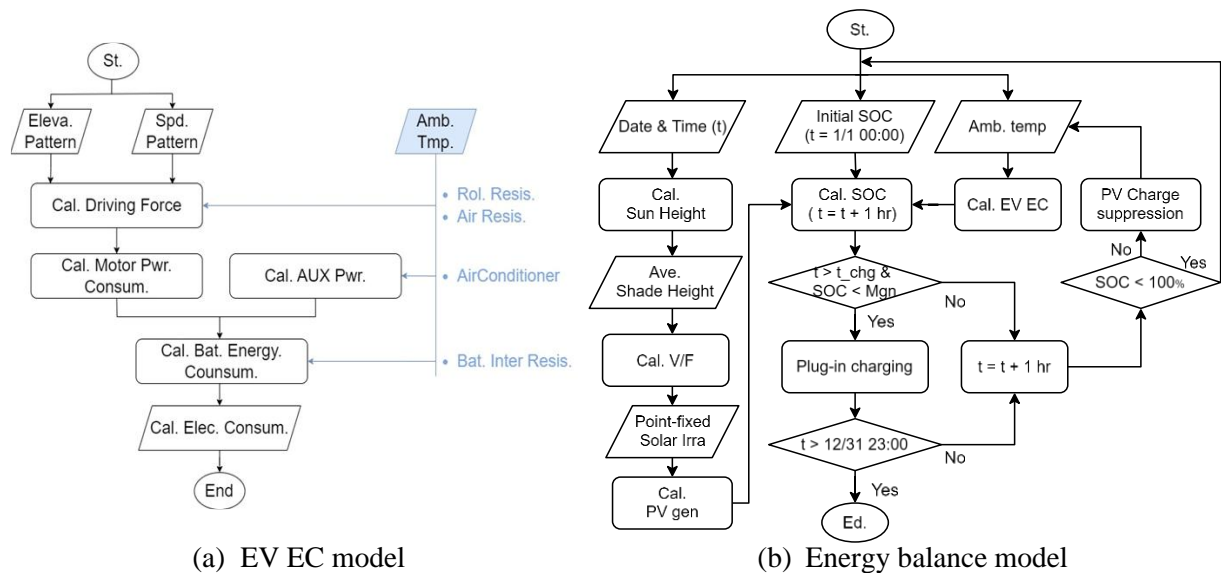   (a) EV EC model   (b) Energy balance model
Figure 9: Overview of simulation model

resistance, and slope resistance. Subsequently, by considering the efficiency of the drivetrain components, the torque, rotational speed, and output power of the motor and inverter are calculated, finally the required electrical energy from the battery is determined. The energy balance model was adapted from a model originally developed for passenger PVEV [5]. Using test data, such as average shade height during parking and driving, temperature, and charging/operation schedules, etc., the model was modified to

suitable for each use case. Fixed-point irradiance was taken from the NEDO (New Energy and Industrial Technology Development Organization, Japan) solar irradiance database METPV-20 [6], where the hourly GHI, DNI, DHI data can be obtained for the common year. Vehicle irradiance was calculated by determining the hourly V/F values based on solar altitude and average shade height. The efficiency of the PV system, the mountable PV area based on vehicle dimensions, PV rated output, and ECU standby power are summarized in the Table 3. The operating conditions assumed day-continuous operation for all 3 use cases over 365 days, and the hourly energy balance was estimated for each of the 8,760 hours in a year. The daily plug-in charging periods and driving time windows were set based on the test data described in Section 2.1. The trips and delivery stops schedule for DVan (KY. Rt.) was also based on the test data. The vehicle is set to begin driving at 13:30, with the following schedule: 13:30–14:00, 3 trips and 2 delivery stops; 14:00–15:00, 5 trips and 6 delivery stops; 15:00–15:30, 3 trips and 2 delivery stops. In total, the daily operation consists of 11 trips, 10 delivery stops, a total driving distance of 14.3 km, and an operation time of 2 hours.

Table 3: PV system main parameters

Items	Unit	CBus (TY. Rt.)	CBus (IO. Rt.)	DVan (KY. Rt.)
PV efficiency	-	20%	20%	20%
PV panel area	m^2	6.0	6.0	2.7
PV Output power	kW	1.2	1.2	0.54
PV system efficiency	-	80.5%	80.5%	80.5%
ECU standby energy [7]	kWh/day	0.12	0.12	0.12

4 Analysis of Impact factors to EV EC and Vehicle Solar Irradiance
4.1 Impact of Temperature and Driving Conditions on EV EC

To investigate the impact of temperature on EV EC rate, driving EC rate and AUX EC rate components were separated from the EVEC rate for each use case, with the results shown in Figure 10. The ratio of the annual average AUX EC rate to the EV EC rate is 24% for CBus (TY. Rt.), 43% for CBus (IO. Rt.), and 59% for DVan (KY. Rt.), indicating a significant influence of AUX in all cases. When temperature varies seasonally, the variation in AUX EC rate is 30~131 Wh/km for CBus (TY. Rt.), 52~206 Wh/km for CBus (IO. Rt.), and 49~311 Wh/km for DVan (KY. Rt.). In contrast, the variation in driving EC rate is 198~244 Wh/km, 130~167 Wh/km, and 109~121 Wh/km for the respective cases. Thus, fluctuations in AUX EC rate are the primary contributors to the large changes in the EVEC rate under varying temperatures.

Regarding the difference of variation magnitude in the AUX EC rate under temperature fluctuations, as addressed in Section 2.2.1, it is strongly correlated with the driving conditions of the different use cases. The larger AUX EC rate variation observed for CBus (IO. Rt.) compared to CBus (TY. Rt.) is attributed to the lower average speed of IO. Rt., which results in a higher AUX EC rate per unit distance. In the case of DVan (KY. Rt.), the greatest variation in AUX EC rate is due to long-time Key-on idling during delivery stops. By switching to Key-off during these stops, AUX EC rate can be suppressed. Figure 11 illustrates that this strategy has the potential to reduce the annual AUX EC rate by 57%. Figure 12 shows the overall reduction in EV EC, with an estimated annual decrease of 33% in EV EC. Notably, during

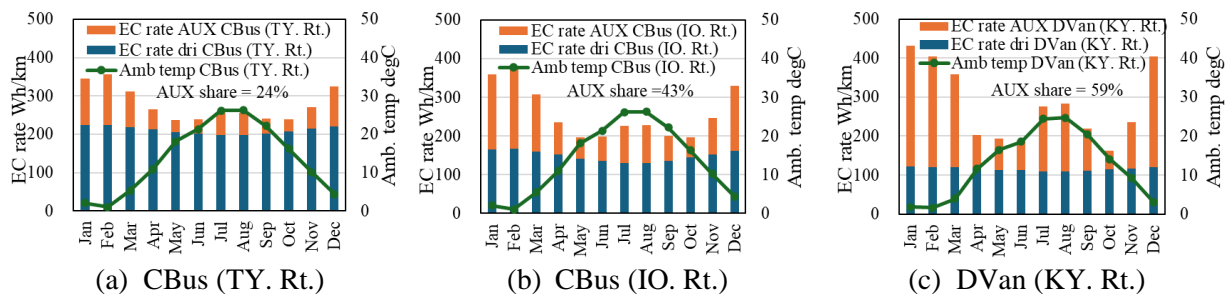(a) CBus (TY. Rt.)   (b) CBus (IO. Rt.)   (c) DVan (KY. Rt.)

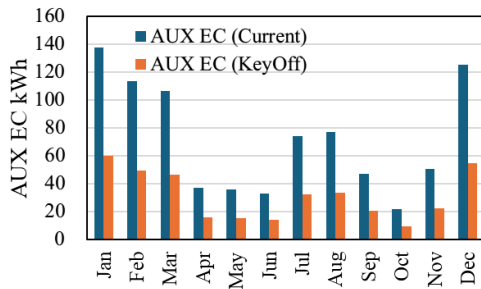Figure 10: EV EC rate for driving and AUX of each use case under different temperature

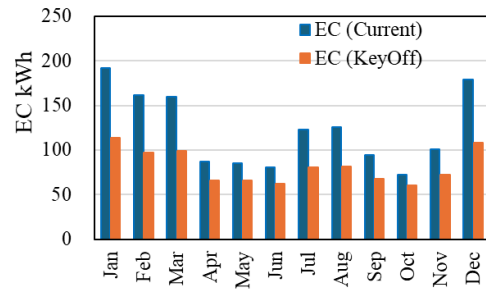Figure 11: AUX EC reduction by key-off

Figure 12: EC reduction by key-off

periods with high air conditioning loads in January and August, reductions of 41% and 35% are estimated. This improvement is expected to enhance the PV installation effect strongly.

Regarding the difference of variation magnitude in the driving EC rate under temperature fluctuations, an analysis was conducted using CBus (TY. Rt.) and CBus (IO. Rt.), which have the same vehicle specifications. The contributions to the driving EC rate, which are the energy for power run by rolling resistance, air resistance, slope resistance, and acceleration resistance, are shown in Figure 13. Ambient temperature affects driving EC rate by influencing rolling and air resistance. But acceleration resistance and slope resistance are independent of ambient temperature, meaning that the EC rate for these components remains unchanged at approximately 172 Wh/km and 88 Wh/km for CBus (TY. Rt.) and CBus (IO. Rt.), regardless of temperature fluctuations. However, the variations in EC rate for rolling resistance and air resistance are 37 Wh/km and 42 Wh/km for CBus (TY. Rt.) and CBus (IO. Rt.), respectively, with the changes in rolling resistance being the primary factor. Since the IO. Rt. exhibits lower slope and acceleration resistance compared to the TY. Rt., the contributions of rolling resistance and air resistance to driving EC rate become relatively more significant, making the driving EC rate more sensitive to ambient temperature changes.
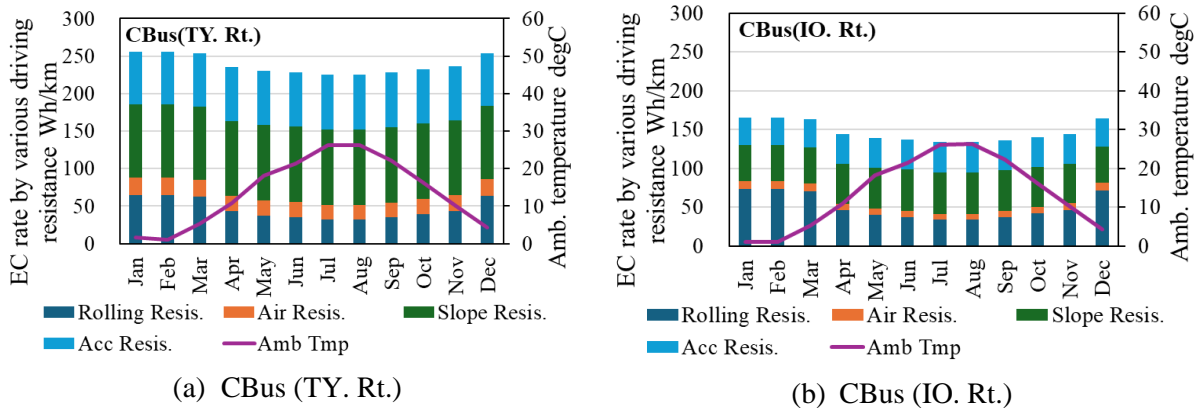

(a) CBus (TY. Rt.)

(b) CBus (IO. Rt.)

Figure 13 Driving EC rate details

4.2 Impact of Driving and Plug-in Charging Time Period on Suppressed PV Power

When the battery is fully charged and the EV EC is low, PV generation cannot be charged into the battery, during which the suppressed PV power occurs. Figure 14 shows an example of suppressed PV power in DVan (KY. Rt.). The battery state-of-charge (SOC) after the previous day's operation (blue line) is approximately 14.5 kWh, and that plug-in charging at 2.5 kW begins at 8:00 AM, the battery reaches 100% within 1 hour (approximately 35 minutes). As a result, PV generation (green line) is halted until the start of operation, and the suppressed PV power occurs in the hatched area. Through Figure 14, we can observe that the amount of suppressed PV power is related to the operation schedule and when the battery SOC becomes 100%. The later the operation begins, the earlier the battery SOC reaches 100%, the more suppressed PV power occurs. To solve this problem and improve the utility rate of PV power, it is necessary to set a plug-in charging margin where the plug-in charging will be forced to stop, to make

room for the PV power generated before operation begins. Figure 15 shows the suppressed PV power for the 3 use cases under different plug-in charging margin conditions. When no plug-in charging margin is set, CBus (TY. Rt.), which has a later departure time than CBus (IO. Rt.), achieves 43.3 kWh of suppressed PV power under favorable irradiance conditions in May, which is 12.4 kWh less than the 30.9 kWh for CBus (IO. Rt.) under the same solar conditions. Although DVan (KY. Rt.) is expected to exhibit the highest suppressed PV power due to its latest departure time, its battery reaches 100% SOC by 8:35, resulting in suppressed PV power of 32.8 kWh, comparable to that of CBus (IO. Rt.). Implementing a plug-in charging margin of 3 kWh for these 3 use cases can eliminate the occurrence of suppressed PV power.
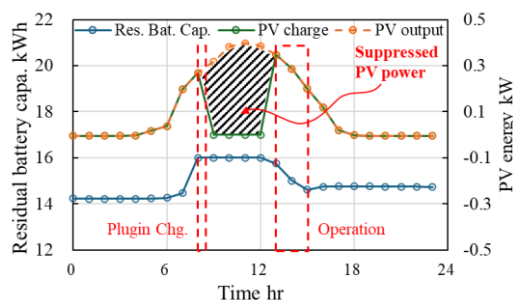

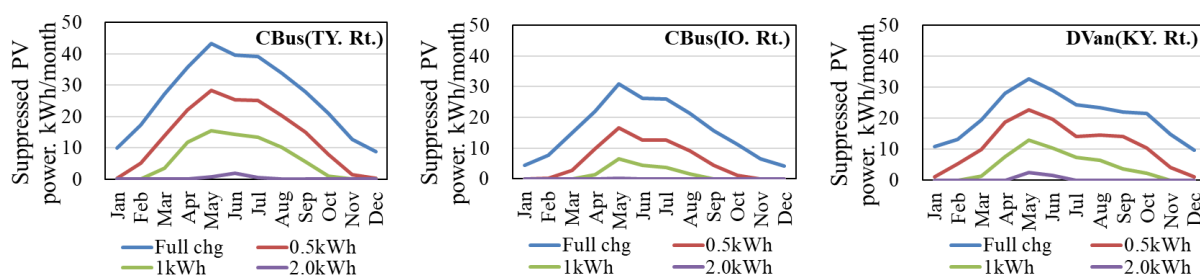Figure 14: Occurrence of suppressed PV power

Figure 15: Suppressed PV power for 3 use cases

5 Estimation of PV Installation Effects on Different Use Cases

Figure 16 and Figure 17 present the monthly EV EC and PV generation for each use case (assuming a charging margin is set such that no PV power is suppressed). Using the PV coverage rate, which is the ratio of PV generation to EVEC, the PV installation effects in different use cases were evaluated, with the results shown in Figure 18. The annual total EVEC for CBus (TY. Rt.), CBus (IO. Rt.), and DVan (KY. Rt.) are 7504 kWh, 3159 kWh, and 1460 kWh, respectively, with PV generation covering 14%, 36%, and 35% of the annual EVEC. In May, when solar conditions are favorable and air-conditioning load is minimal, the PV coverage rates are estimated to reach annual maximums of 25%, 72%, and 78%, respectively. Furthermore, as shown in Figure 19 and discussed in Section 4.1, if DVan (KY. Rt.) switches to a Key-off state during delivery stops, the annual PV coverage rate could be significantly improved from the current 35% to 52%.
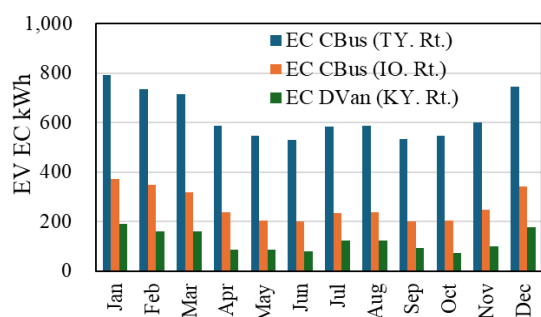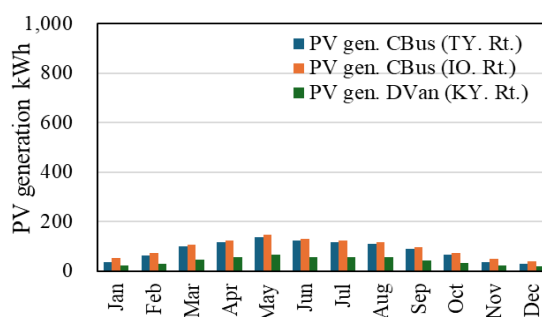

Figure 16: EV EC for 3 use cases
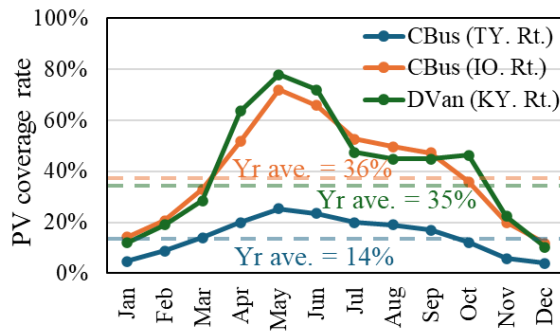

Figure 17: PV generation for 3 use cases
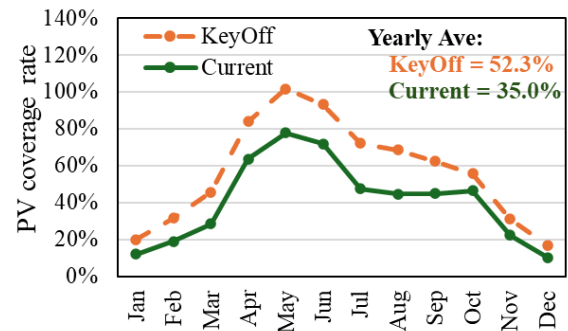
Figure 18: PV installation effects

Figure 19: PV installation effects improvement

6 Summary

(1) EV EC, including AUX EC, is significantly affected by use case and ambient temperature, such as low-speed driving and low ambient temperatures. Particularly, as for DVan (KY. Rt.), EV EC in cold conditions can reach about 3 times high compared to normal temperatures, the primary reason is considered due to much urban driving with low average speeds where rolling resistance has a greater impact, and a high frequency of stops with key-on, heater-on states.

(2) Vehicle irradiance is influenced by shade from surrounding buildings and trees at parking locations and along routes. Vehicle irradiance remains 80~90% of the fixed-point irradiance for DVan (KY. Rt.), benefited from its operation period and the relatively low shade height at parking lot.

(3) Simulation models were developed and the reduction effects of PV system installation for EV EC are estimated. Assuming 365 days of operation, the PV coverage rate, defined as the ratio of the PV generation potential to the EV EC, was estimated. Annually average PV coverage rate for CBus (TY. Rt.) is 14%, it is 36% and 35% for CBus (IO. Rt.) and DVan (KY. Rt.). While in May, with higher irradiance, all of CBus (TY. Rt.), CBus (IO. Rt.), and DVan (KY. Rt.)'s PV coverage rate shows the maximum value of 25%, 72% and 78% respectively throughout the year.

(4) Although the DVan (KY. Rt.)'s daily travel distance is less than half that of the CBus (IO. Rt.), its PV coverage rate is not higher. However, switching to key-off state during delivery stops is estimated to reduce the annual EV EC by 33% and increase the PV coverage rate to 52%.

References

[1] S. Pei, et al, *Feasibility Study of Onboard PV for Commercial Vehicle Application: Analysis on Energy Consumption Reduction Based on Field Test of EV Community Bus*, Transactions of the Society of Automotive Engineers of Japan, ISSN 1883-0811, Vol.55, No. 1, 2024-1

[2] NEDO, *Interim Report of the Study Committee on Vehicles Equipped with Solar Power Generation Systems* https://www.nedo.go.jp/content/100961854.pdf, accessed on 2024-04-07.

[3] IEA PVPS, *State-of-the-Art and Expected Benefits of PV-Powered Vehicles*, https://iea-pvps.org/wp-content/uploads/2021/07/IEA_PVPS_T17_State-of-theart-and-expected-benefits-of-VIPV_report.pdf, access on 2024-04-05

[4] T. Hirota, et al., *Feasibility study of onboard PV for passenger vehicle application: Influence of vehicle irradiance on energy balance of EV energy requirement and PV generation*, Proceedings of the 5th Int'l EV Technology Conference 2021(EVTeC 2021), 20214349, 2021

[5] T. Hirota, et al., *Feasibility study of onboard PV for passenger vehicle application (second report): Feasibility study of onboard PV for passenger vehicle application: Influence of Vehicle Irradiation on Energy Balance of PV Generation and EV Energy Consumption,* Journal of society of Automotive Engineers of Japan, ISSN 1883-0811, Vol.53, No. 4, 2022-7

[6] NEDO, Solar irradiance database METPV-20, https://appww2.infoc.nedo.go.jp/appww/metpv_map.html, access on 2024-12-11

[7] Kimura, K., et al.: *Techno-Economic Analysis of Solar Hybrid Vehicles Part 1: Analysis of Solar Hybrid Vehicle Potential Considering Well-to-Wheel GHG Emissions,* SAE Technical Paper 2016-01-1287, 2016

Presenter Biography

Shuai Pei received his B.Eng. in Mechanics and Aerospace Engineering from Waseda University in 2019 and an M.Eng. from its Graduate School of Environment and Energy Engineering in 2021. Pei is currently pursuing a Ph.D. in Engineering. His research interests include PVEV, vehicle powertrain modeling, EV & HV systems, and EMS control optimization.